1990

Pressure Indication of Twin Screw Compressor

K. Haugland
The Norwegian Institute of Technology

PRESSURE INDICATION OF TWIN SCREW COMPRESSOR

K. Haugland
Division of Refrigeration Engineering
The Norwegian Institute of Technology
N-7034 Trondheim, Norway

ABSTRACT

This paper presents a method for pressure indication of twin screw compressors which have proved to be very robust. Results from various compressor operating conditions are presented.

1. INTRODUCTION

At The Norwegian Institute of Technology we have mainly been working on problems related to reciprocating compressors, especially with problems related to the valves. Five years ago we decided to use the twin screw compressor as a gateway to a better understanding of positive displacement rotary compressors. To achieve this, it was decided to develop a simulation model of twin screw compressors. Verification of such models are very important, and together with other verification methods a pressure indication system was developed, to monitor pressure at different locations in the compressor.

2. PRESSURE INDICATION SYSTEM

Pressure indication is carried out by using five miniature pressure transducers located on the compressor casing along the helical line. Figure 1 shows the transducer locations. Transducers 1, 2 and 3 are mounted radially and transducers 4 and 5 are mounted axially into the compression chambers. The compressor is also equipped with pressure transducers in the suction chamber and in the discharge chamber just outside the outlet port.

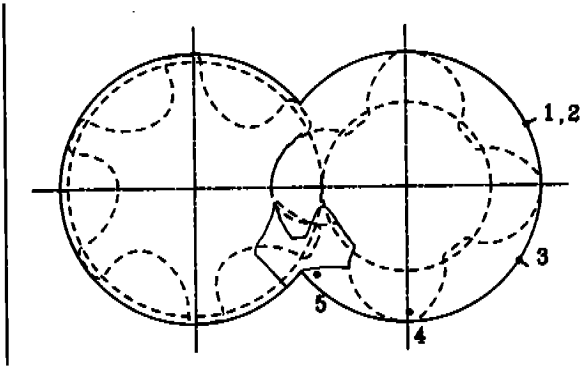

Figure 1 - Principal locations of the pressure transducers. Transducer 2 to 4 is mounted in the discharge end of the compressor. Transducer 1 has the same radial position as transducer 2, but the axial position closer to the suction side.

This arrangement makes it possible to measure about 78% of the compression/discharge process, from α=384° (α-male rotor rotation angle) to α=680°. The compression starts at α=369° and the discharge ends at α=750°. Figure 2 shows an example of the periodical pressure signals from the transducers versus male rotor rotation angle.

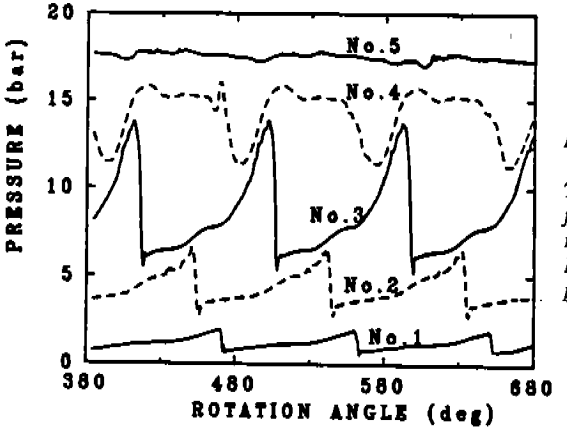

Figure 2

The periodical pressure signals from the transducers versus male rotor rotation angle. For better visibility, the pressure curves are separated.

The signals are assembled to form a pressure curve for one rotor thread. This is done in real time by using an optoelectronic shaft position encoder and a sequencer. The sequencer has an offset compensation module which ensures that the start signal from the next transducer is equal to the last signal from the previous transducer. Finally, the pressure signals are sampled by use of a Personal Computer.

To avoid discontinuities in the pressure curve, the transducers are located in such a way that there is an overlap period between the transducer at the shifting moment. Figure 3 shows the assembling of the pressure curve.

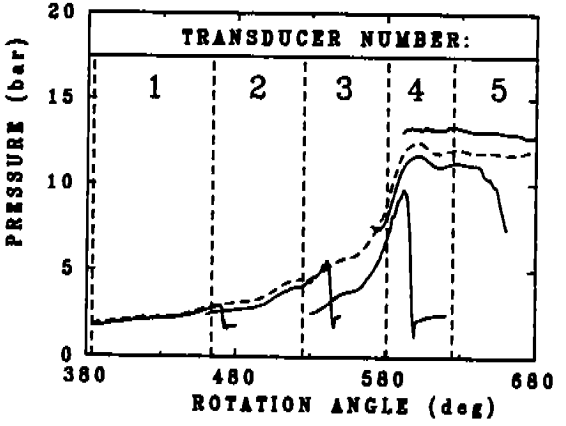

Figure 3 - Assembling of the pressure curve. The broken straight lines show shifting moment. It can be seen from the figure that the transducers are overlapping during the shifting period.

The sample rate of the computer is 33,333 samples/sec. If the compressor speed is 3000 rpm, this means that the sample rate pr degree of main rotor rotation angle is 1.83. This is sufficient to sample the pressure pulsation during discharge.

The pressure transducers are strain gages. The diaphragm is made of stainless steel which make them suitable for ammonia purposes. The resonant frequency of the transducers is 150 kHz and the useful range is linear within +/-5% to 20% of the resonant frequency, which again means that the transducers can measure 1.67 pulsations pr. degree at 3000 rpm.

Time delay while shifting from one transducer to the next is about 7μs (0.09°), an error without any practical significance.

The pressure indication system has proved to be very robust. During the test period of one year we have not had any serious trouble with it. One problem which occured was a drift in the zero offset both randomly and due to temperature changes. The zero offset of the transducers was adjusted by running the compressor to its final temperature, then stopping it and adjusting the zero offset against a calibrated precision manometer. The repeatability is good which can be seen from figure 4 where curves from 6 measurements during a period of 10 minutes are plotted in the same diagram.

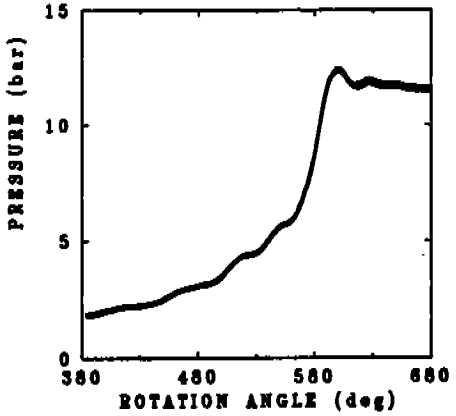

Figure 4 - Repeatability of the pressure indication.

The impact on the transducer at the outlet port is very high due to the oil flow. Hence, it has been difficult to keep this transducer in operation during a longer period. So far, we have destroyed two transducers.

3. RESULTS

A large number of test runs has been done on a oil injected, variable V_i-ratio (built-in volume ratio) compressor. The refrigerant has been ammonia. All the results which are presented in this paper have been run with a condensation temperature of 30°C (11.7 bar).

3.1 Indicator diagrams for built-in volume ratio of 4.0

Figure 5 shows the indicator diagrams for V_i=4.0 for evaporation temperatures from -40 to 0°C (0.72 to 4.30 bar).

With the highest suction pressure a very serious over-compression occurs, and the energy efficiency decreases considerably. Figure 6 gives a comparison of the measured indicator diagram with an isentropic process with the same V_i-ratio. It can be seen that the measured pV-diagram is strongly affected by leakage both to the suction and discharge sides.

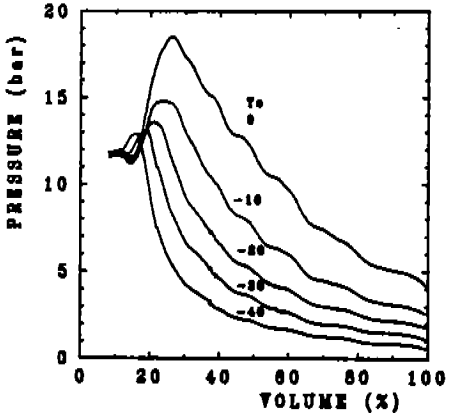

Figure 5 - Indication diagrams for built-in volume ratio of 4.0. The operating pressure ratios vary from 2.7 to 16.0, while the isentropic built - in pressure ratio is about 6.2.

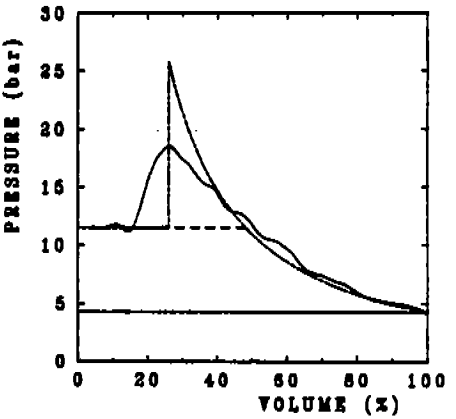

Figure 6 - Measured and isentropic indication diagram for pressure ratio of 2.7. The isentropic pressure peak is two times higher than the measured one.

The indicated work for these two pV-diagrams are nearly the same, although the processes are fundamentally different. Compared to an isentropic process with optimal Vi-ratio, the built-in efficiency is 0.767 for the measured process and 0.800 for the theoretical one.

Influence of discharge pressure on the thread pressure is in this case small, figure 7. Variation of discharge pressure is periodically due to the four male rotor lobes.

Variation of the suction chamber pressure is small, figure 7, and has no significant effect on the compression process. It is periodically due the four male rotor lobes.

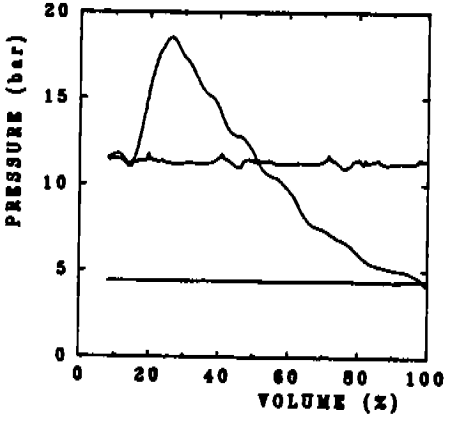

Figure 7 - Pressure variation in suction and discharge chamber.

3.2 Indicator diagrams for built-in volume ratio of 2.6

Indicator diagrams for V_i=2.6 for evaporation temperature from -40 to +10°C (0.72 to 6.16 bar) is given in figure 8.

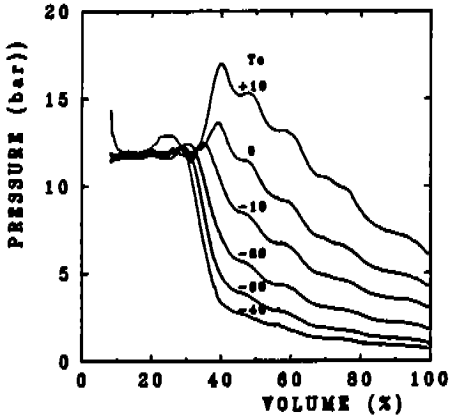

Figure 8 - Indication diagrams for built-in volume ratio of 2.6. The operating pressure ratios varies from 1.9 to 16.0, while the isentropic built-in pressure ratio is about 3.5.

With the lowest suction pressure under-compression is severe, and it is quite clear that the compressor never should be operated under such conditions. However, this mismatch of V_i-ratio is often common when the compressor is operating at part load.

Compared to an isentropic process with the same V_i-ratio, figure 9, the indicated work for the measured process is nearly the same as for the theoretical one. This can be explained in the following manner:

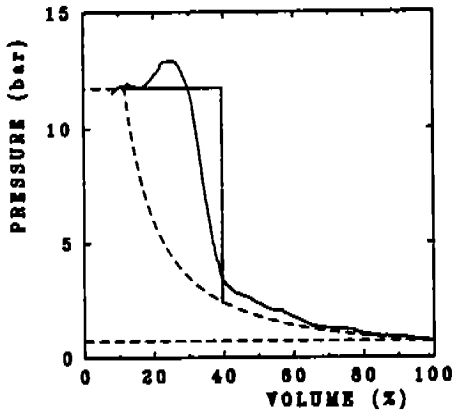

Figure 9 - Measured and isentropic (dashed-dotted line) indication diagram for pressure ratio of 16.0. The isentropic process with optimal V_i-ratio is given by the broken line.

Pressure drop in the discharge port is large during the reverse flow period. Furthermore, the pressure difference between thread pressure and discharge pressure is reduced due to the reversed flow process, figure 10. This reduces back flow and makes the measured process more efficient than the theoretical one. However, because of the leakage flow and the pressure drop during discharge they end up with nearly the same built-in efficiencies. Compared to an isentropic process with optimal V_i-ratio, the efficiency is 0.627 for the measured pV-diagram and 0.602 for the theoretical one.

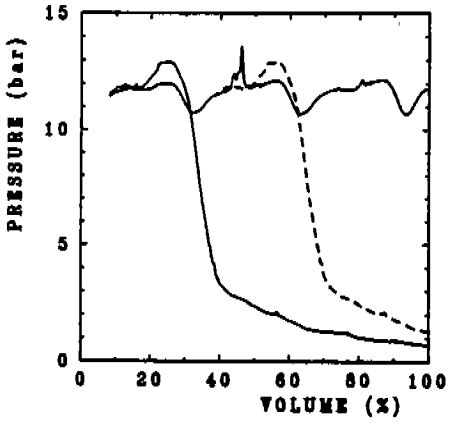

Figure 10 - Pressure variation in discharge chamber for pressure ratio of 16.0. The pressure signal is periodical due to the four male rotor lobes.

The high pressure drop during discharge is caused by the fact that the reversed mass flow also have to be discharged. It can be seen from figure 10 that the reversed flow into one pair of threads has a positive influence on the discharge process of the preceding pair (90° ahead) because discharge chamber pressure is reduced.

3.3 Pressure pulsation during compression

The pressure measurements show rather high pressure pulsation inside the compressor during the compression process. So far we do not know what these pulsation are caused by. It can be noted that an identical pressure pulsation is measured by two pressure transducers when they are in the same thread. The magnitude of the pulsations increases with the suction pressure and the frequency increases when the thread volume decreases. The frequency varies from approximately 350 Hz to 1030 Hz. The frequency is the same regardless of the suction pressure.

3.4 Pressure distribution behind lobes

Information about the leakage flow rate across the lobes may be found by studying the pressure distribution behind the lobes when they sweep the transducers. In figure 11 pressure curves from two adjacent pair of threads are shown together with the pressure distribution in the rotor end clearance which link these threads together.

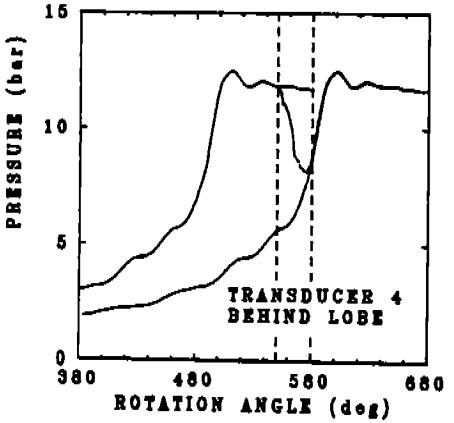

Figure 11 - Pressure distribution behind lobes. V_i=2.6, Pressure ratio=11.6.

When calculating the leakage flow there is one important problem to cope with; the mixture of oil and refrigerant vapor in the clearance is not known. However, some information of this may be found by comparing measured pressure distribution by calculated pressure distribution at different oil flow rate.

4. CHALLENGES

Only a small part of the results which we have sampled have been presented. Analysis of the material have just started. The challenge is to use all this information to get a more fundamental understanding of the many processes that take place inside the screw compressor, and to use this in the development of a simulation model which is more than just an advanced form of curve fitting.

5. ACKNOWLEDGEMENTS

This work was partly supported by The Royal Norwegian Council for Scientific and Industrial Research.